

Cite this: *Dalton Trans.*, 2021, 50, 1740

# An uncoordinated tertiary nitrogen based tricarboxylate calcium network with Lewis acid–base dual catalytic sites for cyanosilylation of aldehydes†

Ying-Xia Wang,<sup>‡</sup> Hui-Min Wang,<sup>‡</sup> Pan Meng, Dong-Xia Song, Juan-Juan Hou  and Xian-Ming Zhang \*

The design and utilization of dual sites for synergistic catalysts has been recognised as an efficient method towards high-efficiency catalysis in the cyanosilylation of aldehydes, which gives key intermediates for the synthesis of a number of valuable natural and pharmaceutical compounds. However, most of the reported dual-site catalysts for this reaction were homogeneous, accompanied by potential deactivation through internal complexation of the dual sites. Herein, by the rational selection of an uncoordinated tertiary nitrogen based tricarboxylic ligand (tris[(4-carboxyl)-phenylduryl]amine, H<sub>3</sub>TCBPA), a new three-dimensional calcium-based metal–organic framework (MOF), Ca<sub>3</sub>(TCBPA)<sub>2</sub>(DMA)<sub>2</sub>(H<sub>2</sub>O)<sub>2</sub> (**1**, where TCBPA = ionized tris [(4-carboxyl)-phenylduryl]amine and DMA = *N,N*-dimethylacetamide), possessing accessible dual catalytic sites, Lewis-basic N and Lewis-acidic Ca, has been designed and constructed by a one-pot solvothermal reaction. As expected, **1** is capable of dually and heterogeneously catalysing the cyanosilylation of aldehydes at room temperature, and can be reused for at least 6 runs with a maximum turnover number (TON) of 1301, which is superior to most reported cases. Additionally, **1** shows CO<sub>2</sub> adsorption ability and conversion with epoxides, which is beneficial for the establishment of a sustainable society.

Received 31st October 2020,  
Accepted 14th December 2020

DOI: 10.1039/d0dt03747h

rsc.li/dalton

## Introduction

Eco-friendliness and high efficiency are extensively pursued by chemists in present-day synthetic organic chemistry.<sup>1</sup> As a result, catalysts with simple operation, high atom efficiency and pleasant catalytic yields are highly desirable.<sup>2–7</sup> Multisite catalysts, especially dual catalytic site catalysts, can stimulate multi-step cascading reactions or improve the catalytic efficiency with their synergistic effects, and thus have been one of the exclusively studied catalytic materials.<sup>8–18</sup> Among the mainly reported catalysts, MOF-based dual catalytic site catalysts have attracted the most considerable attention because of their convenient modification, easy separation, and potential investigation for selectivity and mechanism.<sup>19,20</sup> To date, three types of dual catalytic sites have been mainly

reported for MOF-based catalysts: (1) functionalized ligands with coordinatively unsaturated metal nodes; (2) incorporated active species with active sites on structures; (3) bimetallic nodes. However, most of them were obtained through complicated post-synthetic modification (PSM), which may decrease the pore volume of the initial structures or require detailed confirmation characterization studies.<sup>21–23</sup> Moreover, during the catalytic process, the catalytic sites usually play their roles in successive separate steps, restricting their applications to some extent. Hence, an easy one-pot synthesis of an efficient MOF-based dual-site catalyst, where the two uniformly distributed catalytic sites work simultaneously, is highly desirable.

Cyanosilylation of aldehydes is one of the powerful protocols for the formation of cyanohydrin silyl ethers, key intermediates for high-value  $\beta$ -amino alcohols,  $\alpha$ -hydroxy esters and  $\alpha$ -amino acids.<sup>24–27</sup> Over the past decades, numerous homogeneous or heterogeneous catalysts, including Lewis acids,<sup>28–30</sup> Lewis bases,<sup>31,32</sup> ionic liquids<sup>33</sup> and Lewis acid–base bifunctional catalysts,<sup>34,35</sup> have been extensively applied for the cyanosilylation of aldehydes. However, these catalytic systems have some drawbacks: (i) homogeneous catalysts have high efficiency but difficulty in recovery; (ii) heterogeneous catalysts are easy to separate but present low catalytic efficiency; (iii) Lewis acid–base bifunctional catalysts have superior behavior,

Key Laboratory of Magnetic Molecules and Magnetic Information Materials (Ministry of Education), Institute of Chemistry and Culture, School of Chemistry and Material Science, Shanxi Normal University, Linfen 041004, China.

E-mail: zhangxm@dns.sxnu.edu.cn; Tel: +86 0357 2051402

† Electronic supplementary information (ESI) available. CCDC 2024587. For ESI and crystallographic data in CIF or other electronic format see DOI: 10.1039/d0dt03747h

‡ These authors contributed equally to this work.

but may be diminished through spontaneous internal coordination between flexible Lewis-basic phosphorus, sulfur or oxygen and Lewis-acidic metal. To properly address these issues, we are encouraged to introduce cyanosilylation active Lewis acid and Lewis base catalysts into heterogeneous structures, where the catalytic ability could be maintained, easy recovery could be realized and potential complexation could be limited.

Based on the background hereinbefore and taking the following facts into consideration,  $H_3TCBPA$  is a tridentate carboxylate ligand with a central tertiary Lewis-basic N,<sup>36,37</sup> a potential Lewis base catalyst with steric hindrance for intramolecular coordination; calcium is an Earth-abundant element with strong Lewis acidity,<sup>38,39</sup> high affinity towards oxygen-based ligands<sup>40,41</sup> and a homogeneous catalytic ability for the cyanosilylation of aldehydes.<sup>42</sup> In this work,  $H_3TCBPA$  and  $Ca(OAc)_2$  were chosen as the building units for the construction of a heterogeneous dual catalytic site catalyst through a one-pot solvothermal reaction. As we expected, a stable porous Ca-based MOF formulated as  $[Ca_3(TCBPA)_2(DMA)_2(H_2O)_2]$  (**1**) with accessible Lewis-basic N and Lewis-acidic Ca was obtained and it could catalyze the cyanosilylation of aldehydes effectively at room temperature with a maximum TON of 1301, which is superior to most reported cases. To the best of our knowledge, **1** is the first alkaline-earth element-based MOF with dual catalytic sites for the cyanosilylation of aldehydes. Additionally, **1** has the ability for  $CO_2$  adsorption and further 100% atom-economical cycloaddition with epoxides.

## Results and discussion

The solvothermal reaction of  $Ca(OAc)_2$  with  $H_3TCBPA$  in DMA and  $H_2O$  at 120 °C for 96 h led to the formation of **1** as pale yellow crystals. Single crystal X-ray diffraction revealed that **1** crystallizes in the triclinic space group  $P\bar{1}$ , which contains one TCBPA, two Ca atoms, one coordinated DMA and one  $H_2O$  molecule in the asymmetric unit (Fig. 1a). Ca(1) was hepta-co-

ordinated by six coordinated O atoms from four TCBPA and one from DMA showing a monocapped distorted octahedral geometry (Fig. 1b, left). Different from Ca(1), Ca(2) adopts an octahedral geometry, coordinated with six O atoms, in which the equatorial plane comprised of four carboxylic O atoms and the axial positions were occupied by two water molecules (Fig. 1b, right). Ca(2) is located at the center of symmetry, which connects two Ca(1) atoms by edge-sharing to form a linear trinuclear unit ( $Ca_3$ ). Adjacent  $Ca_3$  units are linked by two carboxyl groups, resulting in a 1D zigzag chain (Fig. 1c). Furthermore, the 1D chains are extended by TCBPA, resulting in a 3D network with two kinds of 1D channels along the  $a$ -axis (Fig. 1d). The window sizes of the channels are approximately  $9.15 \times 16.22 \text{ \AA}^2$  and  $7.43 \times 16.51 \text{ \AA}^2$ . Significantly, the Y-shaped N atoms of TCBPA are exposed to the internal walls, which avoid coordination with the adjacent Ca atom and could act as potential Lewis-basic catalytic sites. Meanwhile, the catalytic ability of Lewis-acidic Ca could be enhanced after removing the coordinated DMA. Under the synergy of the above two effects, **1** could be used as an efficient dual Lewis acid–base catalyst as we expected in the cyanosilylation of aldehydes.

The experimental powder X-ray diffraction (PXRD) pattern (Fig. S3†) of **1** matched well with the simulated one, thus demonstrating the phase purity of the bulk sample and the repeatability of the synthesis method. After immersing in toluene, DCM or acetone for more than 36 h (Fig. S3†), their crystalline structure was maintained well with excellent chemical stability, which is essential for its use as a catalyst in organic synthesis. At the same time, **1** was thermostable (Fig. S4†) with a weight loss in the range of from 100 to 400 °C attributed to the gradual removal of free or coordinated solvent molecules and the collapse temperature was up to 450 °C.

The porosity of **1** was evaluated by  $N_2$  adsorption–desorption isotherms at 77 K. Prior to measurement, fresh samples were activated by solvent exchange with acetone for 4 days (exchanged every 12 h) and heating at 120 °C under vacuum for 12 h. The obtained results (Fig. S5†) showed that **1** exhibited a Type-I isotherm with a maximum adsorption of  $104.51 \text{ m}^3 \text{ g}^{-1}$  and a calculated Langmuir surface area of  $432.08 \text{ m}^2 \text{ g}^{-1}$ . According to the density functional theory (DFT) pore distribution plot (Fig. S6†), **1** exhibited a microporous structure with the main pore width being less than 1 nm, which was consistent with the single crystal data. Additionally, **1** showed  $CO_2$  adsorption ability and the volumetric uptakes were 22.85 and  $36.24 \text{ m}^3 \text{ g}^{-1}$  at 298 K and 273 K, respectively (Fig. S7†).

To test our hypothesis, cyanosilylation of benzaldehyde with  $(CH_3)_3SiCN$  was used as the model reaction to optimize the reaction conditions. As shown in Fig. 2, when cyanosilylation took place in air with 1.2 equivalents of  $(CH_3)_3SiCN$  (column A) in DCM at room temperature, only 20% of **1a** was obtained after 10 h. An inert atmosphere together with a longer time (column B) could improve the yield to 83% but the increment of **1** (column C) had a negligible influence on the reaction. When 2 equivalents of  $(CH_3)_3SiCN$  were used (column D), the yield of **1a** reached up to 100% only after 6 h,

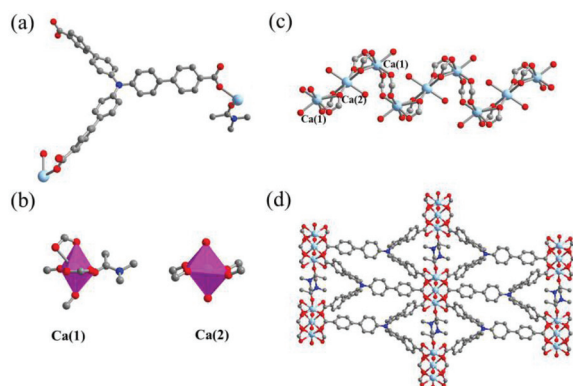


**Fig. 1** (a) Asymmetric unit in **1**. (b) Coordination geometries of Ca(1) (left) and Ca(2) (right). (c) 1D zigzag chain of a  $Ca_3$  unit. (d) 3D network of **1** along the  $a$ -axis.

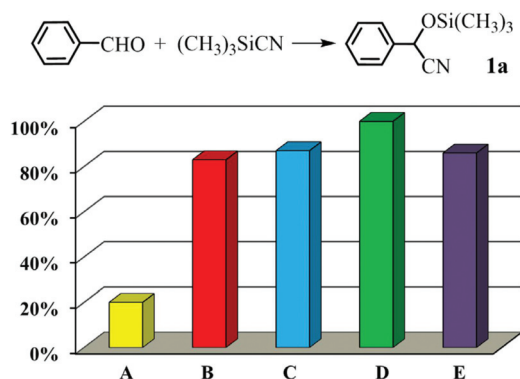


**Fig. 2** Optimization of the reaction conditions. A: benzaldehyde (1 mmol),  $(\text{CH}_3)_3\text{SiCN}$  (1.2 mmol), DCM (4 mL), **1** (5 mg), under an air atmosphere, 10 h; B: the same as A, but under an Ar atmosphere, 12 h; C: the same as B, but 10 mg of **1** was used; D: benzaldehyde (1 mmol),  $(\text{CH}_3)_3\text{SiCN}$  (2 mmol), DCM (4 mL), **1** (5 mg), Ar, 6 h; E: the same as D, but stirred in toluene for 3 h. All of the yields were determined by  $^1\text{H}$  NMR.

indicating that  $(\text{CH}_3)_3\text{SiCN}$  had a great influence on the reaction outcome. The replacement of DCM with toluene (column E) could give **1a** in 86% yield after 3 h, but the larger initial reaction rate (Fig. S8†) and easy handling of DCM prompted us to choose DCM as the optimized solvent. Control experiments in the absence of a catalyst, with  $\text{Ca}(\text{OAc})_2$ ,  $\text{H}_3\text{TCBPA}$  or  $\text{H}_3\text{BTB}$  (1,3,5-tris(4-carboxyphenyl)benzene), were carried out (Table S3, entries 6–9 and Fig. S9†) to determine the exact catalytic active sites. The high yields of **1a** under the catalysis of  $\text{Ca}(\text{OAc})_2$  (99%) and  $\text{H}_3\text{TCBPA}$  (50%), but low yields of **1a** without a catalyst or under the catalysis of  $\text{H}_3\text{BTB}$  revealed that both Lewis-acidic Ca and Lewis-basic N contributed to promoting the reaction, thus confirming the Lewis acid–base dual-site catalytic ability of **1**. Compared to the reported Lewis acid MOF-based catalysts, such as  $\text{Zn}_{0.29}\text{-STU-2}$ ,<sup>43</sup>  $[(\text{Cu}_4\text{O}_{0.27}\text{Cl}_{0.73})_3(\text{H}_{0.5}\text{BTT})_8]$  (BTT = 1,3,5-benzene tristetrazolate),<sup>44</sup>  $[\text{Cd}_2(\text{NiL}^1)(\text{CdL}^2)][\text{Cd}_2(\text{NiL}^1)(\text{H}_2\text{L}^2)]_6\text{DMF}$ . 5MeOH ( $\text{NiL}^1 = (\text{R},\text{R})\text{-N,N}'\text{-bis}(3\text{-tertbutyl-5-(4-pyridyl) salicylidene)-1,2\text{-diphenyldiamine nickel(II)}$ ,  $\text{L}^2 = \text{tetra-(4-carboxy-phenyl)porphyrin}$ ),<sup>45</sup> Ce-MDIP1 ( $\text{H}_4\text{MDIP} = \text{methylenediisophthalic acid}$ ),<sup>46</sup> BINAPDA-Zr-MOF<sup>30</sup> and 1-Cd<sup>47</sup> (Table S4†), dual Lewis acid–base catalyst **1** showed a lower catalyst loading and a shorter reaction time at room temperature.

With the optimal conditions in hand, the general utility of **1** was then explored. As shown in Table 1, a variety of aromatic aldehydes (Table 1, entries 1–8) bearing electron-donating or electron-withdrawing groups could be converted successfully to their corresponding products under the catalysis of **1**; specifically, the yields of **1b–1h** (Table 1, entries 2–8) were 55%, 60%, 94%, 99%, 88%, 92% and 99%, respectively. Further analysis indicated that the electron-withdrawing groups were beneficial for this conversion, as explained by the higher electropositive charge on the carbonyl group. Similar yields of **1g** (Table 1, entry 7) and **1h** (Table 1, entry 8) revealed slight steric hindrance effects. In addition, **1** was applicable

**Table 1** Cyanosilylation of a variety of aldehydes catalyzed by **1**<sup>a</sup>

Entry	Product	Yield/%
1	<b>1a</b>	78
2	<b>1b</b>	55
3	<b>1c</b>	60
4	<b>1d</b>	94
5	<b>1e</b>	99
6	<b>1f</b>	88
7	<b>1g</b>	92
8	<b>1h</b>	99
9	<b>1i</b>	92
10	<b>1j</b>	86
11	<b>1k</b>	55
12	<b>1l</b>	24
13	<b>1m</b>	99
14	<b>1n</b>	99
15 <sup>b</sup>	<b>1a</b>	85

<sup>a</sup> Reaction conditions: Aldehyde (1 mmol),  $(\text{CH}_3)_3\text{SiCN}$  (2 mmol), **1** (5 mg, 0.003 mmol), DCM (4 mL), under an Ar atmosphere, 3 h.  
<sup>b</sup> Reaction conditions: Benzaldehyde (15 mmol),  $(\text{CH}_3)_3\text{SiCN}$  (30 mmol), **1** (5 mg, 0.003 mmol), DCM (60 mL), under an Ar atmosphere, 48 h.

for the cyanosilylation of furfural (Table 1, entry 9), which may poison the catalyst through coordination of the hetero O atom with active Ca, and afforded **1i** with a satisfactory yield of 92%, further proving the existence of dual catalytic sites in **1**. The obtainment of **1j** (Table 1, entry 10) with a yield of 86% indicated a negligible impediment in reaction activity due to the presence of an olefin functional group. The significantly decreased yields of **1k** (Table 1, entry 11) and **1l** (Table 1, entry 12) suggested the bigger the substrates, the lower the catalytic activity.<sup>48</sup> Additionally, the complete conversion of acet-aldehyde and isobutyraldehyde to **1m** (Table 1, entry 13) and **1n** (Table 1, entry 14) proved that **1** was also applicable for the cyanosilylation of aliphatic aldehydes. Finally, for the calculation of maximum TON, **1** was reduced to 0.02 mol%, which gave **1a** in a yield of 85% with a TON of 1301. All of these

results demonstrated the broad applicability of **1** in the cyanosilylation of versatile aromatic and aliphatic aldehydes with  $(\text{CH}_3)_3\text{SiCN}$ .

New portions of reactants were added to the filtrate of the finished reaction to verify the heterogeneity of **1**. After further stirring for 6 h, the yield of **1a** remained unchanged (Fig. S10<sup>†</sup>), which confirmed that this reaction was heterogeneous and almost no homogeneous  $\text{Ca}^{2+}$  was leached into the solution. ICP-OES (inductively coupled plasma optical emission spectroscopy) results showed that the leached  $\text{Ca}^{2+}$  was less than 0.06% of the total Ca content in **1**.

To test our speculation that cyanosilylation occurred not only on the surface but also in the channels of **1**, we recorded the FT-IR spectra (Fig. S11<sup>†</sup>) of **1** before and after overnight immersion in a DCM solution of benzaldehyde or 1-naphthaldehyde. Meanwhile, the  $^1\text{H}$  NMR (Fig. S12<sup>†</sup>) data of the supernatant were obtained by removing **1** from the suspension of DCM with the same molar ratio of benzaldehyde and 1-naphthaldehyde. The appearance of the C=O stretching frequency of aldehyde at  $1700\text{ cm}^{-1}$  for reacquired **1** and the higher concentration of 1-naphthaldehyde than benzaldehyde in the solution suggested that free aldehydes were encapsulated in the channels of **1**, meaning that the cyanosilylation also occurred in the channels of **1**.

Based on the literature reports that either Lewis base or Lewis acid can catalyze the cyanosilylation of aldehyde, along with the coexistence of Lewis-basic N and Lewis-acidic Ca in **1**, a dual activation mechanism for this reaction was tentatively proposed (Fig. 3). In catalytic cycle A, the unsaturated Ca interacted with the oxygen atoms of the aldehydes and polarized the carbonyl groups first. Next, the nucleophilic cyanide was allowed to react with the activated aldehyde carbonyl, affording the target product with the regeneration of **1**. In catalytic cycle B, the electron-rich N in the ligand attacked the vacant 3d orbitals of Si in the  $(\text{CH}_3)_3\text{SiCN}$  and formed a tight ion pair intermediate with hypervalent pentacoordinated Si. After the silyl cation coordination to the aldehyde O and cyanide addition to the positive C, the target product was obtained and **1** was released.

The most attractive advantage of heterogeneous catalysis is easy separation and the reusability of the catalyst. **1** was robust

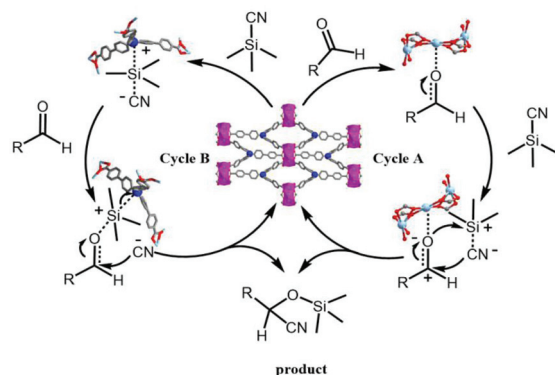


Fig. 3 A plausible reaction mechanism.

in this kind of reaction (Fig. S14<sup>†</sup>) and could be reused for more than 6 runs with high activity. The only operation needed before each repeated run was to wash the recovered **1** with fresh DCM ( $5 \times 8\text{ mL}$ ) and dry it in air.

The ability of **1** for  $\text{CO}_2$  adsorption and the urgency for the solution of the greenhouse effect inspired us to test the catalytic ability of **1** in the conversion of  $\text{CO}_2$  with epoxides.<sup>49</sup> As the attempts indicated, **1** accelerated the reaction only in the presence of TBAB (tetrabutyl ammonium bromide), and an acceptable yield (91%) of **2a** was realized when the reaction took place at  $100\text{ }^\circ\text{C}$  with a  $\text{CO}_2$  balloon for 8 h (Table 2, entries 1–3), comparable to some of the reports from the literature<sup>50–52</sup> (Table S6<sup>†</sup>). Higher yields of **2a** under the conditions of **2d** and **2e** (Table 2, entries 4 and 5) than **2b** (Table 2, entry 2) revealed that the main active site in **1** is  $\text{Ca}^{2+}$ . Under the optimized conditions, the yields of **2b** (Table 2, entry 6) and **2c** (Table 2, entry 7) were 78% and 91%, respectively. Considering the low boiling points of propylene oxide (Table 2, entry 8), 1,2-epoxybutane (Table 2, entry 9) and 1,2-epoxyhexane (Table 2, entry 11), their conversions were performed at room temperature or  $55\text{ }^\circ\text{C}$ , and the corresponding yields of **2d**, **2e** and **2g** were 28%, 18% and 24%, respectively, which show the crucial role of temperature in this reaction.

Table 2 Conversion of  $\text{CO}_2$  with epoxides catalyzed by **1**<sup>a</sup>

Entry	Product	Temperature	Yield/%
1	<b>2a</b>	$100\text{ }^\circ\text{C}$	91
2 <sup>b</sup>	<b>2a</b>	$100\text{ }^\circ\text{C}$	30
3 <sup>c</sup>	<b>2a</b>	$100\text{ }^\circ\text{C}$	0
4 <sup>d</sup>	<b>2a</b>	$100\text{ }^\circ\text{C}$	81
5 <sup>e</sup>	<b>2a</b>	$100\text{ }^\circ\text{C}$	50
6	<b>2b</b>	$100\text{ }^\circ\text{C}$	78
7	<b>2c</b>	$100\text{ }^\circ\text{C}$	91
8	<b>2d</b>	r.t.	28
9 <sup>f</sup>	<b>2e</b>	r.t.	18
10 <sup>f</sup>	<b>2f</b>	$100\text{ }^\circ\text{C}$	17
11	<b>2g</b>	$55\text{ }^\circ\text{C}$	24

<sup>a</sup> Reaction conditions: Epoxides (8.75 mmol), **1** (40 mg, 0.026 mmol), TBAB (40 mg, 0.124 mmol),  $\text{CO}_2$  balloon, 8 h. Yields: based on  $^1\text{H}$  NMR. <sup>b</sup> Epoxides (8.75 mmol), TBAB (40 mg, 0.124 mmol), 8 h. <sup>c</sup> Epoxides (8.75 mmol), **1** (40 mg, 0.026 mmol), 8 h. <sup>d</sup> Epoxides (4.37 mmol),  $\text{Ca}(\text{OAc})_2$  (6 mg, 0.039 mmol), TBAB (20 mg, 0.062 mmol), 8 h. <sup>e</sup> Epoxides (4.37 mmol),  $\text{H}_3\text{TBCPA}$  (24 mg, 0.039 mmol), TBAB (20 mg, 0.062 mmol), 8 h. <sup>f</sup> 24 h.

Additionally, the steric effect may also have a great influence on this reaction, as indicated by the low yield of **2f** of 17% (Table 2, entry 10) even after stirring at 100 °C for 24 h. The unchanged PXRD patterns of **1** after catalysis (Fig. S15†) confirmed that **1** is robust and has an acceptable tolerance in the conversion of CO<sub>2</sub> with epoxides.

## Conclusions

We have designed and synthesized a Ca-based dual catalytic site catalyst **1** using a one-pot strategy for the effective cyanosilylation of aldehydes. Catalytic results illustrated that **1** was heterogeneous and the catalytic process occurred both on the surface and channels of **1**. Meanwhile, **1** could be reused for at least 6 runs without an obvious decrease in catalytic efficiency. Additionally, **1** had the catalytic ability for the conversion of CO<sub>2</sub> with epoxides. We believe that our work will open an avenue for the easy preparation of effective and recyclable catalysts for cyanosilylation of aldehydes.

## Experimental

### General

All reagents were purchased from Energy Chemical and used without further purification. <sup>1</sup>H NMR and <sup>13</sup>C NMR spectra were recorded using a Bruker Avance III DM 600 MHz system. The IR spectra on KBr pellets were obtained using a Nicolet iS50 spectrometer in the region of 4000–400 cm<sup>-1</sup>. PXRD patterns were recorded using a Rigaku D/Max-2500 diffractometer with a Cu target tube at 40 kV and 30 mA. Thermogravimetric analysis (TGA) was performed using a Shanghai yinnuo 1000B system under an N<sub>2</sub> atmosphere at a heating rate of 10 °C min<sup>-1</sup>. The N<sub>2</sub> (77 K) and CO<sub>2</sub> (298 K and 273 K) sorption isotherms were measured using an ASPS 2020 gas sorption analyzer. Scanning electron microscopy energy-dispersive X-ray spectroscopy (SEM-EDS) analyses were conducted using a JSM-7500F SEM equipped with an EDAX CDU leap detector. ICP-OES analysis was performed using a PerkinElmer Optima 8000 Plasma Emission Spectrometer. GC analysis was performed using an Agilent Technologies 7890B GC system.

### Preparation of **1**

Ca(OAc)<sub>2</sub>·H<sub>2</sub>O (12 mg, 0.076 mmol), H<sub>3</sub>TCBPA (9 mg, 0.015 mmol), dimethylacetamide (DMA, 0.6 mL) and H<sub>2</sub>O (0.4 mL) were placed in a 20 mL Teflon-lined stainless steel reactor and were heated at 120 °C in an oven for 4 days. After cooling to room temperature, pale yellow plate crystals were obtained in 73% yield based on the ligand. IR (KBr): 1658 (w), 1600 (s), 1520 (m), 1489 (w), 1405 (s), 1320 (m), 1278 (m), 1183 (m), 1109 (w), 1014 (w), 845 (m), 787 (s), 651 (w), 598 (w), 555 (w).

### X-ray crystallography

Single crystals of **1** were used for intensity data collection using a Bruker SMARTAPEX CCD diffractometer at 298 (2) K

(λ = 0.71073 Å). The structure was solved by direct methods and refined by full-matrix least-squares methods with SHELXTL. All non-hydrogen atoms were refined with anisotropic thermal parameters.

### Typical procedure for cyanosilylation of aldehydes

(CH<sub>3</sub>)<sub>3</sub>SiCN (2 mmol) was added to a mixture of aldehyde (1 mmol) and activated **1** (5 mg, 0.003 mmol) in DCM (4 mL) in a Schlenk tube under an Ar atmosphere. The resulting suspension was stirred at room temperature for 3 h. Then **1** was separated by filtration and the filtrate was evaporated to dryness for <sup>1</sup>H NMR to determine the yield of the corresponding *O*-trimethylsilyl cyanohydrin.

### Experimental procedure for the calculation of maximum TON

(CH<sub>3</sub>)<sub>3</sub>SiCN (30 mmol) was added to the mixture of benzaldehyde (15 mmol) and activated **1** (5 mg, 0.003 mmol) in DCM (60 mL) in a Schlenk bottle under an Ar atmosphere. The resulting suspension was stirred at room temperature for 48 h. Then 1 mL of the reaction mixture was taken out and dried for <sup>1</sup>H NMR to determine the yield of **1a**.

### Typical procedure for cycloaddition of CO<sub>2</sub> with epoxides

Epoxide (8.75 mmol) was added to the Schlenk tube with activated **1** (40 mg, 0.026 mmol) and TBAB (40 mg, 0.124 mmol) under a CO<sub>2</sub> atmosphere. The resulting suspension was stirred at 100 °C with a CO<sub>2</sub> balloon for 8 h. Then, **1** was separated by filtration and the filtrate was used directly for <sup>1</sup>H NMR to determine the yield of the corresponding carbonate.

### Procedure for recycling cyanosilylation of benzaldehyde

The mixture of benzaldehyde (742 mg, 7 mmol) and activated **1** (35 mg, 0.023 mmol) was stirred in DCM (28 mL) at room temperature under an Ar atmosphere. Then (CH<sub>3</sub>)<sub>3</sub>SiCN (1.4 g, 14 mmol) was added and the suspension was stirred for a further 12 h. After that, **1** was collected by centrifugation, washed with fresh DCM (5 × 8 mL), and air-dried for successive runs. The combined supernatant was evaporated to dryness and redissolved in CDCl<sub>3</sub> for <sup>1</sup>H NMR analysis.

## Conflicts of interest

The authors declare no competing financial interests.

## Acknowledgements

This work was supported by the “1331” Project of the Shanxi Province, the Scientific and Technological Innovation Programs of the Higher Education Institutions in Shanxi (2019L0464), the Shanxi Province Science Foundation for Youths (201901D211391), and the Research Project Supported by the Shanxi Scholarship Council of China (2020-088).

## Notes and references

- 1 A. Harinath, J. Bhattacharjee, H. P. Nayek and T. K. Panda, *Dalton Trans.*, 2018, **47**, 12613–12622.
- 2 L. Zhu, X.-Q. Liu, H.-L. Jiang and L.-B. Sun, *Chem. Rev.*, 2017, **117**, 8129–8176.
- 3 Q. Yang, Q. Xu and H.-L. Jiang, *Chem. Soc. Rev.*, 2017, **46**, 4774–4808.
- 4 A. Bavykina, N. Kolobov, I. S. Khan, J. A. Bau, A. Ramirez and J. Gascon, *Chem. Rev.*, 2020, **120**, 8468–8535.
- 5 R. Luo, M. Chen, X. Liu, W. Xu, J. Li, B. Liu and Y. Fang, *J. Mater. Chem. A*, 2020, **8**, 18408–18424.
- 6 N. Sun, C. Wang, H. Wang, L. Yang, P. Jin, W. Zhang and J. Jiang, *Angew. Chem., Int. Ed.*, 2019, **58**, 18011–18016.
- 7 J. Dong, X. Han, Y. Liu, H. Li and Y. Cui, *Angew. Chem., Int. Ed.*, 2020, **59**, 13722–13733.
- 8 Y. Li, Z. Dong and L. Jiao, *Adv. Energy Mater.*, 2019, 1902104–1902139.
- 9 C. M. Wolff, P. D. Frischmann, M. Schulze, B. J. Bohn, R. Wein, P. Livadas, M. T. Carlson, F. Jäckel, J. Feldmann, F. Würthner and J. K. Stolarczyk, *Nat. Energy*, 2018, **3**, 862–869.
- 10 J. Zang, F. Wang, Q. Cheng, G. Wang, L. Ma, C. Chen, L. Yang, Z. Zou, D. Xie and H. Yang, *J. Mater. Chem. A*, 2020, **8**, 3686–3691.
- 11 M. Fang and R. A. Sánchez-Delgado, *J. Catal.*, 2014, **311**, 357–368.
- 12 I. Karakaya, D. N. Primer and G. A. Molander, *Org. Lett.*, 2015, **17**, 3294–3297.
- 13 C.-S. Kwan, A. S. C. Chan and K. C.-F. Leung, *Org. Lett.*, 2016, **18**, 976–979.
- 14 A. Dhakshinamoorthy, Z. Li and H. Garcia, *Chem. Soc. Rev.*, 2018, **47**, 8134–8172.
- 15 R. He, P. Liu, X. Huo and W. Zhang, *Org. Lett.*, 2017, **19**, 5513–5516.
- 16 A. Dhakshinamoorthy and H. Garcia, *ChemSusChem*, 2014, **7**, 2392–2410.
- 17 A. Dhakshinamoorthy, A. M. Asiri and H. Garcia, *Trends Chem.*, 2020, **2**, 452–466.
- 18 A. Das, N. Anbu, M. SK, A. Dhakshinamoorthy and S. Biswas, *Eur. J. Inorg. Chem.*, 2020, 2830–2834.
- 19 Y.-S. Wei, M. Zhang, R. Zou and Q. Xu, *Chem. Rev.*, 2020, **120**, 12089–12174.
- 20 A. Dhakshinamoorthy, A. M. Asiri and H. Garcia, *Catal. Sci. Technol.*, 2016, **6**, 5238–5261.
- 21 Q. Han, B. Qi, W. Ren, C. He, J. Niu and C. Duan, *Nat. Commun.*, 2015, **6**, 10007–10014.
- 22 J. Liang, R.-P. Chen, X.-Y. Wang, T.-T. Liu, X.-S. Wang, Y.-B. Huang and R. Cao, *Chem. Sci.*, 2017, **8**, 1570–1575.
- 23 T.-T. Liu, J. Liang, Y.-B. Huang and R. Cao, *Chem. Commun.*, 2016, **52**, 13288–13291.
- 24 N. Kurono and T. Ohkuma, *ACS Catal.*, 2016, **6**, 989–1023.
- 25 W. Wang, M. Luo, W. Yao, M. Ma, S. A. Pullarkat, L. Xu and P.-H. Leung, *ACS Sustainable Chem. Eng.*, 2019, **7**, 1718–1722.
- 26 J. Amaro-Gahete, D. Esquivel, J. R. Ruiz, C. Jiménez-Sanchidrián and F. J. Romero-Salguero, *Appl. Catal., A*, 2019, **585**, 117190–117197.
- 27 M. K. Sharma, D. Singh, P. Mahawar, R. Yadav and S. Nagendran, *Dalton Trans.*, 2018, **47**, 5943–5947.
- 28 Z. Zhang, H. Y. Bae, J. Guin, C. Rabalakos, M. van Gemmeren, M. Leutzsch, M. Klusmann and B. List, *Nat. Commun.*, 2016, **7**, 12478–12485.
- 29 S. Rawat, M. Bhandari, B. Prashanth and S. Singh, *ChemCatChem*, 2020, **12**, 2407–2411.
- 30 F.-Z. Jin, C.-C. Zhao, H.-C. Ma, G.-J. Chen and Y.-B. Dong, *Inorg. Chem.*, 2019, **58**, 9253–9259.
- 31 Y.-L. Zhao, Z.-Y. Cao, X.-P. Zeng, J.-M. Shi, Y.-H. Yu and J. Zhou, *Chem. Commun.*, 2016, **52**, 3943–3946.
- 32 Z. Zhang, M. Klusmann and B. List, *Synlett*, 2020, **31**, 1–5.
- 33 Z. Meng, M. Zhang and H. Yang, *Green Chem.*, 2019, **21**, 627–633.
- 34 M. Hatano, K. Yamakawa, T. Kawai, T. Horibe and K. Ishihara, *Angew. Chem., Int. Ed.*, 2016, **55**, 4021–4025.
- 35 Q.-W. Yu, L.-P. Wu, T.-C. Kang, J. Xie, F. Sha and X.-Y. Wu, *Eur. J. Org. Chem.*, 2018, 3992–3996.
- 36 Y.-P. He, Y.-X. Tan and J. Zhang, *Inorg. Chem.*, 2015, **54**, 6653–6656.
- 37 K. S. Lim, S. Y. Jeong, D. W. Kang, J. H. Song, H. Jo, W. R. Lee, W. J. Phang, D. Moon and C. S. Hong, *Chem. – Eur. J.*, 2017, **23**, 4803–4809.
- 38 M. K. Sharma, S. Sinhababu, G. Mukherjee, G. Rajaraman and S. Nagendran, *Dalton Trans.*, 2017, **46**, 7672–7676.
- 39 N. Xu, Q. Zhang, B. Hou, Q. Cheng and G. Zhang, *Inorg. Chem.*, 2018, **57**, 13330–13340.
- 40 S.-L. Cai, Z.-H. He, W.-H. Wu, F.-X. Liu, X.-L. Huang, S.-R. Zheng, J. Fan and W.-G. Zhang, *CrystEngComm*, 2017, **19**, 3003–3016.
- 41 Y. Tang, A. C. Soares, M. Ferbinteanu, Y. Gao, G. Rothenberg and S. Tanase, *Dalton Trans.*, 2018, **47**, 10071–10079.
- 42 S. Yadav, R. Dixit, K. Vanka and S. S. Sen, *Chem. – Eur. J.*, 2018, **24**, 1269–1273.
- 43 J.-J. Du, X. Zhang, X.-P. Zhou and D. Li, *Inorg. Chem. Front.*, 2018, **5**, 2772–2776.
- 44 L.-J. Zhang, C.-Y. Han, Q.-Q. Dang, Y.-H. Wang and X.-M. Zhang, *RSC Adv.*, 2015, **5**, 24293–24298.
- 45 J. Li, Y. Ren, C. Qi and H. Jiang, *Chem. Commun.*, 2017, **53**, 8223–8226.
- 46 D. Dong, P. Wu, C. He, Z. Xie and C. Duan, *J. Am. Chem. Soc.*, 2010, **132**, 14321–14323.
- 47 W. Jiang, J. Yang, Y.-Y. Liu, S.-Y. Song and J.-F. Ma, *Inorg. Chem.*, 2017, **56**, 3036–3043.
- 48 A. Dhakshinamoorthy, H. Garcia and A. M. Asiri, *ChemCatChem*, 2020, **12**, 4732–4753.
- 49 W.-G. Cui, G.-Y. Zhang, T.-L. Hu and X.-H. Bu, *Coord. Chem. Rev.*, 2019, **387**, 79–120.
- 50 S. Cheng, Y. Wu, J. Jin, J. Liu, D. Wu, G. Yang and Y.-Y. Wang, *Dalton Trans.*, 2019, **48**, 7612–7618.
- 51 A. Helal, M. Usman, M. E. Arafat and M. M. Abdelnaby, *J. Ind. Eng. Chem.*, 2020, **89**, 104–110.
- 52 Z. Xue, J. Jiang, M.-G. Ma, M.-F. Li and T. Mu, *ACS Sustainable Chem. Eng.*, 2017, **5**, 2623–2631.